

# Pressure-induced phase coexistence in $\text{BaFe}_{1.8}\text{Co}_{0.2}\text{As}_2$

Ling-Yun Tang,<sup>1,2</sup> Qian Tao,<sup>3</sup> Zhu-An Xu,<sup>3</sup> and Xiao-Jia Chen<sup>2,4,a)</sup><sup>1</sup>Department of Physics, South China University of Technology, Guangzhou 510640, China<sup>2</sup>Center for High Pressure Science and Technology Advanced Research, Shanghai 201203, China<sup>3</sup>Department of Physics, Zhejiang University, Hangzhou 310027, China<sup>4</sup>Geophysical Laboratory, Carnegie Institution of Washington, Washington, DC 20015, USA

(Received 28 January 2014; accepted 28 March 2014; published online 11 April 2014)

We report high-pressure powder synchrotron X-ray diffraction measurements of overdoped  $\text{BaFe}_{1.8}\text{Co}_{0.2}\text{As}_2$  under quasi-hydrostatic pressure up to 40.1 GPa. Our results indicate that a tetragonal (T) to collapsed tetragonal (CT) phase transition occurs at 16.8 GPa and the two phase coexist until 30 GPa, which has not been previously observed in iron arsenide compounds. Both the lattice parameters  $a$  and  $c$  show discontinuous change for the T and CT phases. The decrease of the  $c$  lattice parameter is as large as 12.2% owing to the uniaxial pressure effect. The axial ratio  $c/a$  of the T phase exhibits similar features to the other 122-type compounds below 16.8 GPa, whereas there is a very small increase with increasing pressure in the two phase coexistence region. Because of the relationship between the axial ratio and superconductivity, the abnormal expansion may be related to the sudden increase of the strength of antiferromagnetic spin fluctuations. © 2014 AIP Publishing LLC. [<http://dx.doi.org/10.1063/1.4870860>]

## I. INTRODUCTION

In the iron-arsenide-based superconductors, the 122-type  $\text{AFe}_2\text{As}_2$  ( $A = \text{Ba}, \text{Ca}, \text{Sr}, \text{or Eu}$ ) family has attracted great interest because of their unique properties.  $\text{BaFe}_2\text{As}_2$  is the common parent compound with a tetragonal (T) structure (space group  $I4/mmm$ ) and is non-superconducting at ambient pressure but exhibits a tetragonal to orthorhombic phase transition associated with magnetic ordering from the paramagnetic to the antiferromagnetic (AF) state at low temperature.<sup>1,2</sup> The orthorhombic phase with AF ordering can be suppressed by chemical substitution or pressure, and then superconductivity develops. Electron doping via cobalt substitution in  $\text{Ba}(\text{Fe}_{1-x}\text{Co}_x)_2\text{As}_2$  compounds are probably the most well-studied systems because of the availability of high-quality single crystals. Superconductivity with this type of dopant exhibits the dome shape in certain doping regions.<sup>3,4</sup> In the underdoped region, various experiments<sup>3-5</sup> have revealed that the structural/magnetic phase transitions are gradually suppressed and the superconducting temperature ( $T_c$ ) increases with increasing Co concentration. These phenomena indicate that there is competition between superconductivity and antiferromagnetism.<sup>6</sup> In-plane resistivity measurements have shown that the anisotropy in resistivity arises because of impurity scattering by Co atoms substituted in Fe sites, and the magnitude increases for  $0 \leq x \leq 0.04$  and then decreases before disappearing above the optimal doping level ( $x \approx 0.06$ ).<sup>7</sup> However, in the overdoped region, the structural/magnetic transitions are totally suppressed. This makes the physical properties of the overdoped compounds different from the underdoped compounds.<sup>8</sup> The superconductivity was proposed to be associated with the strength of spin fluctuations and Fermi surface nesting.<sup>9-13</sup> The structure of the Fermi surface markedly changes by

increasing the doping level.<sup>14-16</sup> A Lifshitz transition occurs at a doping of  $x \approx 0.1$  with an ellipsoid centered at the Brillouin zone (Z), and this Z ellipsoid disappears and the central pocket becomes electron-like above  $x \approx 0.2$ , which is another Lifshitz transition, and the superconductivity completely disappears.<sup>16</sup>

Pressure plays an important role in superconductivity as a cleaning parameter without introducing the disorder effect. For Co substitution, the effect of pressure on the superconductivity depends on the doping level. Transport measurements<sup>17-19</sup> have shown that  $T_c$  is strongly enhanced in underdoped compounds, for example,  $T_c$  at  $x \approx 0.041$  increases from 11 to 25 K by the application of pressure.<sup>17</sup> In contrast, overdoped materials show very little increase in  $T_c$  by applying pressure.<sup>17</sup> Most of the studies on Co substitution have focused on the properties at low pressures before the absence of superconductivity. In fact, a non-magnetic collapsed tetragonal structure is observed in the parent compound and the superconductivity disappears under pressure.<sup>20</sup> In addition, a second superconducting phase has been found in the 122\*-type iron-based superconductors with a higher  $T_c$  than that in the first superconducting phase after it disappeared.<sup>21</sup> A detailed understanding of the properties of these compounds at high pressure is therefore of particular importance.

In this study, we chose the overdoped material  $\text{BaFe}_{1.8}\text{Co}_{0.2}\text{As}_2$  for the experiments because of its unique properties mentioned above. We investigated the structural properties of this overdoped material at pressures up to 40.1 GPa. Coexistence of the low-pressure T phase and the high-pressure collapsed tetragonal (CT) phase occurs, which is observed for the first time for the 122 iron arsenide compounds. The axial ratio  $c/a$  is not continuous but increases after passing through a minimum. This behavior indicates a potential reemergence of superconductivity owing to the enhancement of the AF spin fluctuations at high pressures.

<sup>a)</sup>Electronic mail: xjchen@ciw.edu

## II. EXPERIMENTAL DETAILS

A single crystal sample of  $\text{BaFe}_{1.8}\text{Co}_{0.2}\text{As}_2$  was grown by the self-flux method with high-purity elements Ba, Fe, and Co using FeAs as the flux. The detailed procedure for synthesizing the samples has been reported previously.<sup>22</sup> The X-ray powder diffraction measurements were carried out at the 4W2 beam line of the Beijing Synchrotron Radiation Facility (BSRF). The wavelength of the X-ray radiation was 0.6199 Å. An applied pressure was generated by a symmetric diamond anvil cell with 300  $\mu\text{m}$  culet size anvils. A stainless steel gasket preindented to  $\sim 40\ \mu\text{m}$  with a central hole of 120  $\mu\text{m}$  in diameter was used as the sample chamber. The powder sample ground from single crystals was loaded into the chamber with silicon oil as the pressure-transmitting medium. The pressure was determined by the shift of the fluorescence line of the ruby.<sup>23</sup> The sample to image plate (MAR345) detector distance was refined using the diffraction data of  $\text{CeO}_2$  standard. The two-dimensional powder images were integrated using the program FIT2D<sup>24</sup> to give the intensity versus  $2\theta$  plot. The structural fits were performed using GSAS.<sup>25</sup>

## III. RESULTS AND DISCUSSION

Typical angle dispersive powder X-ray diffraction data collected for  $\text{BaFe}_{1.8}\text{Co}_{0.2}\text{As}_2$  at various pressures and room temperature are shown in Fig. 1. The left part of Fig. 1 shows a portion of the diffraction patterns at selected pressures during the pressure increasing cycle. At the lowest pressure (0.9 GPa), the X-ray diffraction pattern corresponds to the T phase, which has been identified for other doped and undoped 122-type compounds. Upon compression above 16.8 GPa, the diffraction profiles show a dramatic change. A new peak appears on the left shoulder of the (103) peak, and the Bragg peaks at around  $2\theta = 17.5^\circ$  and  $18.5^\circ$  converge and then merge, indicating the onset of a structural transition.

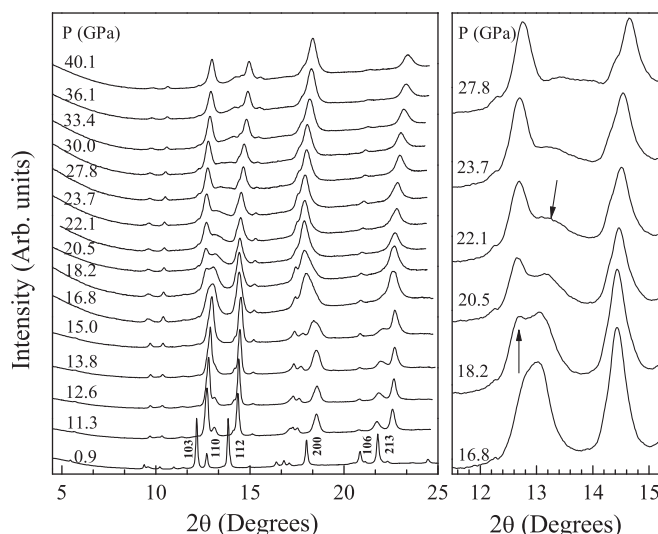


FIG. 1. X-ray diffraction patterns of  $\text{BaFe}_{1.8}\text{Co}_{0.2}\text{As}_2$  for various pressures at room temperature (left panel). The enlargement of the diffraction patterns for 16.8–27.8 GPa with  $2\theta$  from  $11^\circ$  to  $15^\circ$  (right panel) shows the structural transition with two coexisting phases. The up arrow indicates the emerging peak, while the down arrow indicates the disappearing peak.

In the pressure range 16.8–30 GPa, the intensity of the (103) peak decreases while that of the new peak increases. This indicates the coexistence of the low-pressure T and high-pressure phases. The phase transition is complete after the (103) peak disappears at 30 GPa and the high-pressure phase remains stable up to 40.1 GPa. The right part of Fig. 1 shows an enlargement of the peaks from  $2\theta = 11^\circ$ – $15^\circ$  at pressures ranging from 16.8 to 27.8 GPa, and the competition between the intensities of the (103) peak (down arrow) and the new peak (up arrow) of the high-pressure phase is clearly shown.

As previously mentioned, a first-order phase transition from the T phase to the CT phase has been found in 122-type iron arsenide materials under pressure.<sup>26–28</sup> We refined the diffraction patterns above 30 GPa for the CT phase, and one of the fitting results is shown in the top panel of Fig. 2. The result is quite reasonable for the high-pressure CT phase. In addition, we refined the patterns in the pressure region from 16.8 to 30 GPa for the T and CT phases, and the refinement and experimental data for 20.5 GPa are in good agreement. This provides the evidence for the coexistence of both the low-pressure and high-pressure phases as mentioned above. Therefore, a transition from the T to the CT phase occurs at high pressure with an intermediate region with the coexistence of the two phases. This observation is different from that of the parent compound.<sup>20,28</sup> In the parent compound  $\text{BaFe}_2\text{As}_2$ , the diffraction patterns can be indexed to the single tetragonal structure over the whole pressure range even during the transition process.<sup>20</sup> Carefully comparing the diffraction patterns obtained in this study with the diffraction patterns of the overdoped compound  $\text{BaFe}_{1.84}\text{Ni}_{0.16}\text{As}_2$ ,<sup>29</sup> we found that a similar phase coexistence could occur in the Ni-doped compounds, although the existence is not as obvious as in this study. It seems that the coexistence of the T and CT phases is a universal phenomenon in the overdoped regime.

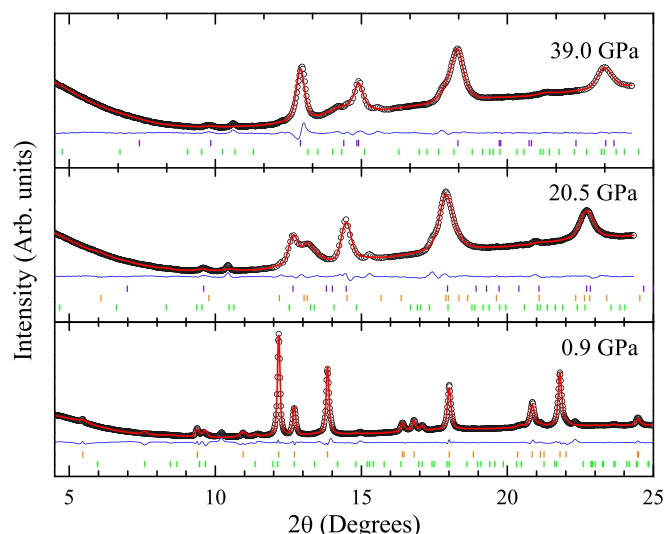


FIG. 2. Observed (black open circles) and calculated (red line) X-ray diffraction patterns, and the difference between the observed and calculated profiles after fitting (blue line). The bottom panel is obtained with the T phase, the middle panel with both the low- and high-pressure phases, and the top panel with the CT phase.

In Fig. 3, we show the pressure dependence of the lattice parameters  $a$  and  $c$ , and both show distinct changes. A clear decrease in the lattice parameter  $c$  (as large as 12.2%) and a 4.4% increase of lattice parameter  $a$  are observed at 16.8 GPa. This clearly shows that a structural transition from the T to the CT phase occurs for this compound. The large decrease in  $c$  is ascribed to As–As hybridization in 122-type compounds,<sup>30</sup> i.e., the As ion below the top Fe-plane forms a bond with the As ion above the lower Fe-plane, with the loss of Fe-magnetic momentum. Therefore, the collapse transition from the T to the CT phase is also a magnetic transition from a paramagnetic to a nonmagnetic state, in which the total energy difference between the two states is compensated by the formation of a new As–As bond. Upon forming the CT phase, the previously weakly connected FeAs layers are pulled together and the As–As bond strength increases. The crossing mirror plane As–As bonding would decrease the Fe–As bond strength by altering the Fe–As bond angles and increasing the lattice parameter,  $a$  as observed in the present experiments. In the parent compound BaFe<sub>2</sub>As<sub>2</sub>, the decrease in  $c$  is 4.9% with He as the pressure transmitting medium,<sup>28</sup> but 15.5% with no pressure transmitting medium.<sup>27</sup> The decrease of the lattice parameter  $c$  in this study with silicon oil as the pressure medium is slightly smaller than that with no pressure medium. Thus, the reason for the larger decrease in  $c$  in this material compared with BaFe<sub>2</sub>As<sub>2</sub> may be because of the uniaxial pressure effect. However, the abrupt changes of the lattice parameters  $a$  and  $c$  are very different from those of the parent compound, in which the lattice parameter  $a$  exhibits intermediate anomalous expansion with a  $S$  shape and  $c$  gradually decreases at high pressures.<sup>20</sup> From the results of 122-type compounds in the literature, such abrupt changes were ascribed to the different types of electrons in Eu-compounds, i.e., the changes in EuFe<sub>2</sub>As<sub>2</sub> were continuous, but in EuCo<sub>2</sub>As<sub>2</sub> and EuNi<sub>2</sub>As<sub>2</sub> they exhibited strongly discontinuous features.<sup>31</sup> Conversely, in the undoped and underdoped CaFe<sub>2</sub>As<sub>2</sub> compounds, the distinct abrupt changes were observed under pressure and/or

at low temperature because the smaller size of Ca results in the two FeAs layers being much closer than in Ba-based compounds, which is beneficial for the formation of the As–As bond.<sup>32,33</sup> It has been found<sup>19</sup> that the Co doping effect can induce the decrease of the distance between the FeAs layers. Nevertheless, these studies indicate that Co doping should account for the abrupt change of the lattice parameters, although more evidence is required to figure out how the Co doping works in the overdoped region.

With regard to the pressure dependence of the lattice parameters, in the case of the two phase coexistence region,  $a$  and  $c$  show different pressure dependence in the T and CT phases. It is worth noting that  $c$  of the T phase is almost unchanged, whereas  $a$  shows a slight decrease in the two phase coexistence region. The changes of the two lattice parameters result in a slight increase of the axial ratio, as shown in Fig. 4. This probably indicates a second-order phase transition. Density functional theory calculations<sup>30</sup> predicted that the phase transforms to a nonmagnetic T phase and then to a nonmagnetic CT phase in Ba-compounds, but the nonmagnetic T phase has not been observed in experiments.

To obtain more insight into the structural properties, we examined the axial ratio as a function of pressure shown in Fig. 4. The axial ratio exhibits different features in the three regimes. Below 16.8 GPa in the pure T phase, the axial ratio is almost constant below 6 GPa and then rapidly decreases with increasing pressure until the critical transition point. The  $c/a$  axial ratio has been found<sup>19</sup> to be closely related to the superconductivity, especially the  $T_c$ , as reported in 122-type iron-based compounds previously. Hence, the  $T_c$  of the Co-dopant in this study may maintain a relatively high value up to 6 GPa, and then decrease as the pressure is increased. In fact, similar variation of  $T_c$  as a function of pressure has been observed in the sister BaFe<sub>1.9</sub>Ni<sub>0.1</sub>As<sub>2</sub> compound in electronic transport experiments.<sup>34</sup> Upon further compression, the axial ratio abruptly changes by as much as 7.4% between the T phase and CT phases. In the pressure range from 16.8 to 30 GPa for the coexistence, the axial ratio monotonically decreases in the CT phase but only exhibits a

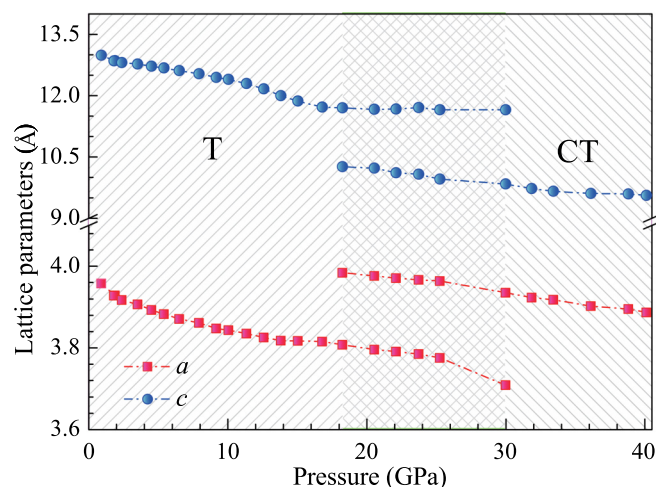


FIG. 3. Lattice parameters  $a$  (red solid squares) and  $c$  (blue solid circles) of BaFe<sub>1.8</sub>Co<sub>0.2</sub>As<sub>2</sub> as a function of pressure.  $a$  increases abruptly and  $c$  exhibits a large decrease at 18.7 GPa, which indicates the onset of the transition from T phase to CT phase.

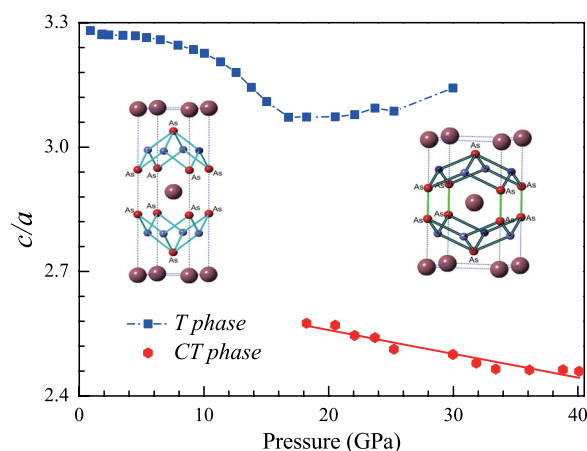


FIG. 4. Axial ratio  $c/a$  for the low- and high-pressure phases of BaFe<sub>1.8</sub>Co<sub>0.2</sub>As<sub>2</sub> as a function of pressure up to 40.1 GPa. The solid line is the linear fitting results of the data in the CT phase.



very small increase in the T phase with increasing pressure. The axial ratio of the CT phase continues linearly decreasing up to 40.1 GPa. This is similar to other 122-type compounds. We fitted the data as a function of pressure and obtained the linear equation  $c/a = 2.673 - 0.006P$ , which is almost the same as that in the parent compound.<sup>35</sup>

Figure 5 shows the pressure dependence of the unit cell volume ( $V$ ) of  $\text{BaFe}_{1.8}\text{Co}_{0.2}\text{As}_2$  at room temperature. We separately fitted the pressure–volume data using the third-order Birch–Murnaghan equation of state<sup>36</sup> at fixed  $B'_0 = 4$  for the pressure ranges 0.9–15 GPa (T phase) and 18.2–40.1 GPa (CT phase). The fitted ambient pressure volumes  $V_0$  were  $204.9(0.7) \text{ \AA}^3$  for the T phase, which agrees well with reported values for the parent material,<sup>20</sup> and  $196.4(2.7) \text{ \AA}^3$  for the CT phase. The measured equation of state shows considerable stiffening at the tetragonal to collapsed tetragonal phase transition, as evidenced by the change in the slope of the volume–pressure curve at 16.8 GPa in Fig. 5. Based on the measured data, the transition is first-order with a volume change as large as 3.7%. The obtained values of the bulk modulus were  $B_0 = 66.3(2.7) \text{ GPa}$  for the T phase and  $B_0 = 69.5(5.1) \text{ GPa}$  for the CT phase. This indicates that the CT phase is less incompressible than the T phase. The  $B_0$  of the CT phase in this material was only about 45% of the value of the parent  $\text{BaFe}_2\text{As}_2$  material,<sup>28</sup> whereas the  $B_0$  values in the T phase of both compounds are almost the same. The large discrepancy of the  $B_0$  values in the CT phase is probably because of the different  $B'_0$  values ( $B'_0 = 1.8$  in  $\text{BaFe}_2\text{As}_2$ ).<sup>28</sup> Therefore, we refitted the data of the CT phase of  $\text{BaFe}_{1.8}\text{Co}_{0.2}\text{As}_2$  by setting  $B'_0 = 1.8$  and obtained  $B_0 = 141.9(5.1) \text{ GPa}$ , which is close to the  $B_0$  value of the parent compound (153 GPa).

The decrease of  $T_c$  or superconductivity in 122-type compounds has been suggested to result from the suppression of the AF spin fluctuations, and thus the decrease of the effective mass  $m^*$ .<sup>13,34,37</sup> As previously reported in optimally doped and overdoped  $\text{BaFe}_{2-x}\text{Ni}_x\text{As}_2$ , AF spin fluctuations were found to substantially decrease with increasing pressure, and the decrease of the  $T_c$  was also observed with

pressure.<sup>38</sup> Magnetic measurements of optimally doped  $\text{BaFe}_2(\text{As}_{0.65}\text{P}_{0.35})_2$  suggested that the decrease of  $m^*$  could account for the  $T_c$  decrease with pressure.<sup>39</sup> As the  $T_c$  is strongly related to the structure and magnetism, the axial ratio should be correlated with the AF spin fluctuations. Thus, our observed decrease of the axial ratio indicates a decrease of AF spin fluctuation and a decrease of  $m^*$  and superconductivity under pressures above 6 GPa.

With increasing pressure, an isostructural transformation from a T phase to a CT phase occurs and the superconductivity disappears. The large decrease of the axial ratio in the CT phase reflects the strong suppression of AF spin fluctuations, which has been observed in  $\text{CaFe}_2\text{As}_2$  by high pressure inelastic scattering measurements.<sup>40</sup> Although the same transition from the T to the CT phase is observed in this material, the coexistence of the two phases occurs before complete phase transition. This behavior has not been observed in the 122-compounds.<sup>20,28,41–43</sup> Moreover, the axial ratio of the T phase slightly increases with pressure when the T phase coexists with the CT phase. Since the decrease of the axial ratio of the T phase corresponds to suppression of the AF spin fluctuations and a decrease of  $m^*$ , the increase of the axial ratio may reflect variations of the AF spin fluctuations and  $m^*$ , i.e., the increase of the strength of the AF spin fluctuations. It is an intriguing finding because it indicates that there may be a second superconducting phase under pressure. In fact, a second superconducting phase has been found in the 122\*-type iron base superconductors and has a relatively high  $T_c$  compared to the first superconducting phase.<sup>21</sup> Further experiments are required, such as resistivity measurements, to verify this finding.

For  $\text{Ba}(\text{Fe}_{1-x}\text{Co}_x)_2\text{As}_2$  system, the Fermi surface topology has been proposed to be an important factor for the superconductivity.<sup>14–16</sup> The shape of the Fermi surface at the doping level ( $x = 0.2$ ) for this studied compound is an ellipsoid centered at Z, which is a result of a Lifshitz transition due to the doping effects.<sup>16</sup> Upon increasing the doping level, this Z ellipsoid shrinks in size until it disappears accompanied by the central pocket becoming electron-like, which marks another Lifshitz transition, and the superconductivity disappears. Pressure should have a similar effect as doping because of the similarity between overdoping and pressure. Thus, the Lifshitz transition could also occur at the some critical pressure in this studied compound.

#### IV. CONCLUSIONS

We have performed high-pressure X-ray diffraction measurements of  $\text{BaFe}_{1.8}\text{Co}_{0.2}\text{As}_2$  up to 40.1 GPa. Our results revealed that a T to CT phase transition occurs at 16.8 GPa. Unlike the parent compound, the two phases coexist at pressures ranging from 16.8 to 30 GPa before formation of the pure CT phase. Because of the Co doping effect, both  $a$  and  $c$  exhibit abrupt changes when the phase transition occurs. The large difference in  $c$  between the two phases suggests the importance of the uniaxial pressure effect. The  $c/a$  axial ratio of the T phase slightly increased in the two phase coexistence region. The slight difference of the axial ratio may indicate a new superconducting phase because of

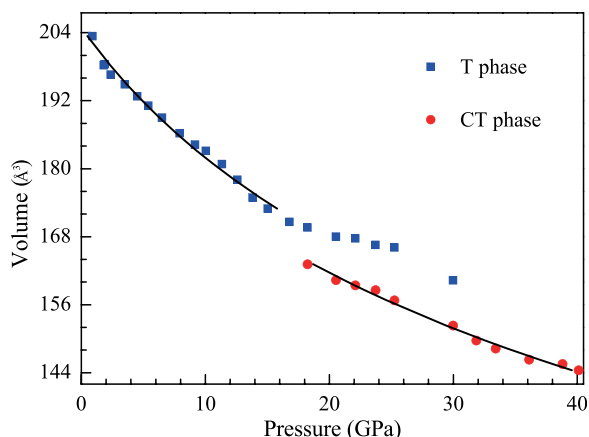


FIG. 5. Equations of state for the tetragonal (T) and collapsed tetragonal (CT) phases of  $\text{BaFe}_{1.8}\text{Co}_{0.2}\text{As}_2$  for pressures up to 40.1 GPa. The blue solid squares and red solid circles represent the experimental data for the T phase and CT phase, respectively. The solid black curves are the fitting results of the two phases with the third-order Birch–Murnaghan equation.

the possible enhancement of the AF spin fluctuations at high pressures.

## ACKNOWLEDGMENTS

The work at the Carnegie Institution was supported by EFree, an Energy Frontier Research Center funded by DOE-BES under Grant No. DE-SC0001057. The work in China was supported by the China 973 Program (Grant No. 2011CBA00103), NSFC (Grant No. 11174247), the Cultivation Fund of the Key Scientific, and Technical Innovation Project Ministry of Education of China (No. 708070), Guangdong Natural Science Foundation (No. S2012040007929), and the Fundamental Research Funds for the Central Universities SCUT (No. D213235w). 4W2 beam-line at the BSRF was supported by CAS (Grant Nos. KJCX2-SW-N20 and KJCX2-SW-N03).

- <sup>1</sup>A. S. Sefat, R. Jin, M. A. McGuire, B. C. Sales, D. J. Singh, and D. Mandrus, *Phys. Rev. Lett.* **101**, 117004 (2008).
- <sup>2</sup>M. G. Kim, R. M. Fernandes, A. Kreyssig, J. W. Kim, A. Thaler, S. L. Bud'ko, P. C. Canfield, R. J. McQueeney, J. Schmalian, and A. I. Goldman, *Phys. Rev. B* **83**, 134522 (2011).
- <sup>3</sup>S. Nandi, M. G. Kim, A. Kreyssig, R. M. Fernandes, D. K. Pratt, A. Thaler, N. Ni, S. L. Bud'ko, P. C. Canfield, J. Schmalian, R. J. McQueeney, and A. I. Goldman, *Phys. Rev. Lett.* **104**, 057006 (2010).
- <sup>4</sup>J. H. Chu, J. G. Analytis, C. Kuncharczyk, and I. R. Fisher, *Phys. Rev. B* **79**, 014506 (2009).
- <sup>5</sup>X. F. Wang, T. Wu, G. Wu, R. H. Liu, H. Chen, Y. L. Xie, and X. H. Chen, *New J. Phys.* **11**, 045003 (2009).
- <sup>6</sup>L. Fang, H. Luo, P. Cheng, Z. Wang, Y. Jia, G. Mu, B. Shen, I. I. Mazin, L. Shan, C. Ren, and H. H. Wen, *Phys. Rev. B* **80**, 140508(R) (2009).
- <sup>7</sup>S. Ishida, M. Nakajima, T. Liang, K. Kihou, C. H. Lee, A. Iyo, H. Eisaki, T. Kakeshita, Y. Tomioka, T. Ito, and S. Uchida, *Phys. Rev. Lett.* **110**, 207001 (2013).
- <sup>8</sup>K. Matan, S. Ibuka, R. Morinaga, S. Chi, J. W. Lynn, A. D. Christianson, M. D. Lumsden, and T. J. Sato, *Phys. Rev. B* **82**, 054515 (2010).
- <sup>9</sup>K. Terashima, Y. Sekiba, J. H. Bowen, K. Nakayama, T. Kawahara, T. Sato, P. Richard, Y. M. Xu, L. J. Li, G. H. Cao, Z. A. Xu, H. Ding, and T. Takahashi, *Proc. Natl. Acad. Sci. U.S.A.* **106**, 7330 (2009).
- <sup>10</sup>A. N. Yaresko, G. Q. Liu, V. N. Antonov, and O. K. Andersen, *Phys. Rev. B* **79**, 144421 (2009).
- <sup>11</sup>J. G. Analytis, J. H. Chu, R. D. McDonald, S. C. Riggs, and I. R. Fisher, *Phys. Rev. Lett.* **105**, 207004 (2010).
- <sup>12</sup>S. Arsenijevic, H. Hodovanets, R. Gaal, L. Forro, S. L. Bud'ko, and P. C. Canfield, *Phys. Rev. B* **87**, 224508 (2013).
- <sup>13</sup>G. F. Ji, J. S. Zhang, L. Ma, P. Fan, P. S. Wang, J. Dai, G. T. Tan, Y. Song, C. L. Zhang, P. C. Dai, B. Normand, and W. Q. Yu, *Phys. Rev. Lett.* **111**, 107004 (2013).
- <sup>14</sup>P. Vilmercati, A. Fedorov, I. Vobornik, U. Manju, G. Panaccione, A. Goldoni, A. S. Sefat, M. A. McGuire, B. C. Sales, R. Jin, D. Mandrus, D. J. Singh, and N. Mannella, *Phys. Rev. B* **79**, 220503(R) (2009).
- <sup>15</sup>C. Liu, T. Kondo, R. M. Fernandes, A. D. Palczewski, E. D. Mun, N. Ni, A. N. Thaler, A. Bostwick, E. Rotenberg, J. Schmalian, S. L. Bud'ko, P. C. Canfield, and A. Kaminski, *Nat. Phys.* **6**, 419 (2010).
- <sup>16</sup>C. Liu, A. D. Palczewski, R. S. Dhaka, T. Kondo, R. M. Fernandes, E. D. Mun, H. Hodovanets, A. N. Thaler, J. Schmalian, S. L. Bud'ko, P. C. Canfield, and A. Kaminski, *Phys. Rev. B* **84**, 020509(R) (2011).
- <sup>17</sup>K. Ahilan, J. Balasubramanian, F. L. Ning, T. Imai, A. S. Sefat, R. Jin, M. A. McGuire, B. C. Sales, and D. Mandrus, *J. Phys.: Condens. Matter* **20**, 472201 (2008).
- <sup>18</sup>K. Ahilan, F. L. Ning, T. Imai, A. S. Sefat, M. A. McGuire, B. C. Sales, and D. Mandrus, *Phys. Rev. B* **79**, 214520 (2009).
- <sup>19</sup>S. Drotziger, P. Schiweiss, K. Grube, T. Wolf, P. Adelman, C. Meingast, and H. V. Lohneysen, *J. Phys. Soc. Jpn.* **79**, 124705 (2010).
- <sup>20</sup>W. G. Yang, F. J. Jia, L. Y. Tang, Q. Tao, Z. A. Xu, and X. J. Chen, *J. Appl. Phys.* **115**, 083915 (2014).
- <sup>21</sup>L. L. Sun, X. J. Chen, J. Guo, P. W. Gao, Q.-Z. Huang, H. D. Wang, M. H. Fang, X. L. Chen, G. F. Chen, Q. Wu, C. Zhang, D. C. Gu, X. L. Dong, L. Wang, K. Yang, A. G. Li, X. Dai, H.-K. Mao, and Z. X. Zhao, *Nature (London)* **483**, 67 (2012).
- <sup>22</sup>L. J. Li, Y. K. Luo, Q. B. Wang, H. Chen, Z. Ren, Q. Tao, Y. K. Li, X. Lin, M. He, Z. W. Zhu, G. H. Cao, and Z. A. Xu, *New J. Phys.* **11**, 025008 (2009).
- <sup>23</sup>H. K. Mao, J. Xu, and P. M. Bell, *J. Geophys. Res.* **91**, 4673, doi:10.1029/JB091iB05p04673 (1986).
- <sup>24</sup>A. P. Hammersley, S. O. Svensson, M. Hanfland, A. N. Fitch, and D. Hausermann, *High Pressure Res.* **14**, 235 (1996).
- <sup>25</sup>A. C. Larson and R. B. Von-Dreele, "GSAS-General Structure Analysis System," Report No. LAUR 86-748, Los Alamos National Laboratory, USA, 1994.
- <sup>26</sup>J. E. Jorgensen, J. S. Olsen, and L. Gerward, *Solid State Commun.* **149**, 1161 (2009).
- <sup>27</sup>W. Uhoya, A. Stemshorn, G. Tsoi, Y. K. Vohra, A. S. Sefat, B. C. Sales, K. M. Hope, and S. T. Weir, *Phys. Rev. B* **82**, 144118 (2010).
- <sup>28</sup>R. Mittal, S. K. Mishra, S. L. Chaplot, S. V. Ovsyannikov, E. Greenberg, D. M. Trots, L. Dubrovinsky, Y. Su, Th. Brueckel, S. Matsuishi, H. Hosono, and G. Garbarino, *Phys. Rev. B* **83**, 054503 (2011).
- <sup>29</sup>F. J. Jia, W. G. Yang, L. J. Li, Z. A. Xu, and X. J. Chen, *Physica C* **474**, 1 (2012).
- <sup>30</sup>W. Ji, X.-W. Yan, and Z.-Y. Lu, *Phys. Rev. B* **83**, 132504 (2011).
- <sup>31</sup>C. Huhnt, W. Schlabit, A. Wurth, A. Mewis, and M. Reehuis, *Physica B* **252**, 44 (1998).
- <sup>32</sup>S. Kasahara, T. Shibauchi, K. Hashimoto, Y. Nakai, H. Ikeda, T. Terashima, and Y. Matsuda, *Phys. Rev. B* **83**, 060505 (2011).
- <sup>33</sup>A. Kreyssig, M. A. Green, Y. Lee, G. D. Samolyuk, P. Zajdel, J. W. Lynn, S. L. Bud'ko, M. S. Torikachvili, N. Ni, S. Nandi, J. B. Leao, S. J. Poulton, D. N. Argyriou, B. N. Harmon, R. J. McQueeney, P. C. Canfield, and A. I. Goldman, *Phys. Rev. B* **78**, 184517 (2008).
- <sup>34</sup>X. J. Chen, F. J. Jia, J. B. Zhang, Z. X. Qin, L. Y. Tang, Q. Tao, Z. A. Xu, J. Liu, V. V. Struzhkin, R. E. Cohen, and H. K. Mao, e-print arXiv:1209.6028v1.
- <sup>35</sup>J. R. Jeffries, N. P. Butch, K. Kirshenbaum, S. R. Saha, G. Samudrala, S. T. Weir, Y. K. Vohra, and J. Paglione, *Phys. Rev. B* **85**, 184501 (2012).
- <sup>36</sup>F. Birch, *Phys. Rev.* **71**, 809 (1947).
- <sup>37</sup>T. Imai, K. Ahilan, F. L. Ning, T. M. McQueen, and R. J. Cava, *Phys. Rev. Lett.* **102**, 177005 (2009).
- <sup>38</sup>X. D. Zhang, G. Z. Fan, C. L. Zhang, X. N. Jing, and J. L. Luo, *Chin. Phys. Lett.* **29**, 017401 (2012).
- <sup>39</sup>S. K. Goh, Y. Nakaj, K. Ishida, L. E. Klitberg, Y. Ihara, S. Kasahara, T. Shibauchi, Y. Matsuda, and T. Terashima, *Phys. Rev. B* **82**, 094502 (2010).
- <sup>40</sup>D. K. Pratt, Y. Zhao, S. A. J. Kimber, A. Hiess, D. N. Argyriou, C. Broholm, A. Kreyssig, S. Nandi, S. L. Bud'ko, N. Ni, P. C. Canfield, R. J. McQueeney, and A. I. Goldman, *Phys. Rev. B* **79**, 060510(R) (2009).
- <sup>41</sup>W. O. Uhoya, J. M. Montgomery, G. M. Tsoi, Y. K. Vohra, M. A. McGuire, A. S. Sefat, B. C. Sales, and S. T. Weir, *J. Phys.: Condens. Matter* **23**, 122201 (2011).
- <sup>42</sup>M. Bishop, W. Uhoya, G. Tsoi, Y. K. Vohra, A. S. Sefat, and B. C. Sales, *J. Phys.: Condens. Matter* **22**, 425701 (2010).
- <sup>43</sup>W. O. Uhoya, G. M. Tsoi, Y. K. Vohra, M. A. McGuire, and A. S. Sefat, *J. Phys.: Condens. Matter* **23**, 365703 (2011).